



Visualization and Analysis of Impact Damage in Sapphire

by Elmar Strassburger, Parimal Patel, and James W. McCauley

ARL-RP-345

November 2011

*A reprint from the Proceedings of the 26th International Symposium on Ballistics,
Miami, FL, 12–16 September 2011.*

NOTICES

Disclaimers

The findings in this report are not to be construed as an official Department of the Army position unless so designated by other authorized documents.

Citation of manufacturer's or trade names does not constitute an official endorsement or approval of the use thereof.

Destroy this report when it is no longer needed. Do not return it to the originator.

Army Research Laboratory

Aberdeen Proving Ground, MD 21005-5066

ARL-RP-345**November 2011**

Visualization and Analysis of Impact Damage in Sapphire

Elmar Strassburger

Fraunhofer-Institut für Kurzzeiddynamik, Ernst-Mach-Institut (EMI)

Parimal Patel and James W. McCauley

Weapons and Materials Research Directorate, ARL

*A reprint from the Proceedings of the 26th International Symposium on Ballistics,
Miami, FL, 12–16 September 2011.*

REPORT DOCUMENTATION PAGE				Form Approved OMB No. 0704-0188	
Public reporting burden for this collection of information is estimated to average 1 hour per response, including the time for reviewing instructions, searching existing data sources, gathering and maintaining the data needed, and completing and reviewing the collection information. Send comments regarding this burden estimate or any other aspect of this collection of information, including suggestions for reducing the burden, to Department of Defense, Washington Headquarters Services, Directorate for Information Operations and Reports (0704-0188), 1215 Jefferson Davis Highway, Suite 1204, Arlington, VA 22202-4302. Respondents should be aware that notwithstanding any other provision of law, no person shall be subject to any penalty for failing to comply with a collection of information if it does not display a currently valid OMB control number. PLEASE DO NOT RETURN YOUR FORM TO THE ABOVE ADDRESS.					
1. REPORT DATE (DD-MM-YYYY) November 2011		2. REPORT TYPE Reprint		3. DATES COVERED (From - To) 12-16 September 2011	
4. TITLE AND SUBTITLE Visualization and Analysis of Impact Damage in Sapphire				5a. CONTRACT NUMBER CA W911NF-09-1-0335	
				5b. GRANT NUMBER	
				5c. PROGRAM ELEMENT NUMBER	
6. AUTHOR(S) Elmar Strassburger,* Parimal Patel, and James W. McCauley				5d. PROJECT NUMBER	
				5e. TASK NUMBER	
				5f. WORK UNIT NUMBER	
7. PERFORMING ORGANIZATION NAME(S) AND ADDRESS(ES) U.S. Army Research Laboratory ATTN: RDRL-WM Aberdeen Proving Ground, MD 21005-5066				8. PERFORMING ORGANIZATION REPORT NUMBER ARL-RP-345	
9. SPONSORING/MONITORING AGENCY NAME(S) AND ADDRESS(ES)				10. SPONSOR/MONITOR'S ACRONYM(S)	
				11. SPONSOR/MONITOR'S REPORT NUMBER(S)	
12. DISTRIBUTION/AVAILABILITY STATEMENT Approved for public release; distribution is unlimited.					
13. SUPPLEMENTARY NOTES A reprint from the <i>Proceedings of the 26th International Symposium on Ballistics</i> , Miami, FL, 12-16 September 2011. *Fraunhofer-Institut für Kurzezeitdynamik, Ernst-Mach-Institut (EMI), Am Christianswuh 2, 79400 Kandern, Germany					
14. ABSTRACT This report reviews work carried out with the fully instrumented Edge-on Impact (EOI) facility at the Ernst-Mach-Institute (EMI), using a Cranz-Schardin high speed camera, modified for dynamic photoelasticity, to quantify stress wave propagation, damage nucleation and propagation during high velocity impacts. The experimental technique has been used to examine monolithic single crystal sapphire plates (100 mm x 100 mm x 10 mm) in crystallographically controlled directions impacted at about 400 m/s with both steel solid cylinders and spheres. The plates were impacted as follows: 100 mm x 100 mm large surface r-plane parallel to the a-axis; large surface a-plane parallel and perpendicular to the c-axis; large surface c-plane parallel to a-axis; and impacting perpendicular to r-plane small surface. In certain orientations damage propagation is clearly by macro-cleavage with significant cleavage branching. The velocities of damage and cleavage propagation are presented.					
15. SUBJECT TERMS sapphire, impact, damage, cleavage					
16. SECURITY CLASSIFICATION OF:			17. LIMITATION OF ABSTRACT UU	18. NUMBER OF PAGES 22	19a. NAME OF RESPONSIBLE PERSON James W. McCauley
a. REPORT Unclassified	b. ABSTRACT Unclassified	c. THIS PAGE Unclassified			19b. TELEPHONE NUMBER (Include area code) 410-306-0711

This paper reviews work carried out with the fully instrumented Edge-on Impact (EOI) facility at the Ernst-Mach-Institute (EMI), using a Cranz-Schardin high speed camera, modified for dynamic photoelasticity, to quantify stress wave propagation, damage nucleation and propagation during high velocity impacts. The experimental technique has been used to examine monolithic single crystal sapphire plates (100 mm x 100 mm x 10 mm) in crystallographically controlled directions impacted at about 400 m/s with both steel solid cylinders and spheres. The plates were impacted as follows: 100 mm x 100 mm large surface r-plane parallel to the a-axis; large surface a-plane parallel and perpendicular to the c-axis; large surface c-plane parallel to a-axis; and impacting perpendicular to r-plane small surface. In certain orientations damage propagation is clearly by macro-cleavage with significant cleavage branching. The velocities of damage and cleavage propagation are presented.

INTRODUCTION

It has been demonstrated that significant weight reductions can be achieved compared to conventional glass-based armor when a transparent ceramic is used as strike face on a glass-polymer laminate [1, 2, 3]. Sapphire, i.e. single crystal aluminum oxide, is one of the candidate materials for use as a hard front layer in transparent armor [4, 5]. Due to the high number of influencing parameters, a detailed understanding of the dominant mechanisms during projectile penetration is required in order to improve the performance of multi-layer, ceramic faced transparent armor. On one hand, a high ballistic resistance is related to projectile deformation and erosion. On the other hand, the resistance to penetration, and therefore the ability to deform and erode the projectile, depends on the damage and failure mechanisms in the target materials. Since part of transparent armor consists

of brittle materials, the fragmentation of the ceramic and glass layers plays a key role in the resistance to penetration [6, 7].

A series of studies has been conducted in the last years in order to visualize damage initiation and propagation in transparent armor materials like Starphire® soda-lime and borosilicate glass [8], fused silica [9] and the transparent polycrystalline ceramic AlON [10].

EXPERIMENTAL

An Edge-on Impact (EOI) test method coupled with a high speed Cranz-Schardin camera, with frame rates up to 10^7 fps, has been developed at the Fraunhofer-Institute for High-Speed Dynamics, EMI, to visualize damage propagation and dynamic fracture in structural ceramics. Two different optical configurations were employed. A regular transmitted light shadowgraph set-up was used to observe wave and damage propagation and a modified configuration, where the specimens were placed between crossed polarizers and the photo-elastic effect was utilized to visualize the stress waves. Impact tests at approximately equivalent velocities were carried out in transmitted plane (shadowgraphs) and crossed polarized light. Figure 1 shows a schematic of the Edge-on Impact test with the added crossed polarizers; Figure 2 illustrates an exploded view of the impactor/sample interaction. Both steel solid cylinder (mass 127 g, diameter 30 mm) and spherical impactors (mass 39.1 g, diameter 15.9 mm) have been used at a velocity of ≈ 400 m/s on 100 mm x 100 mm x 10 mm plates.

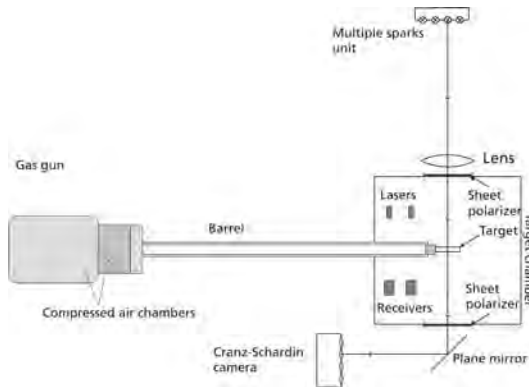


Fig. 1: EOI Test Set-up with Cranz-Schardin camera

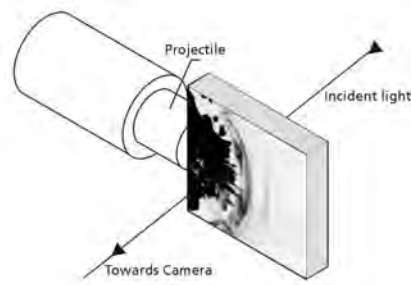


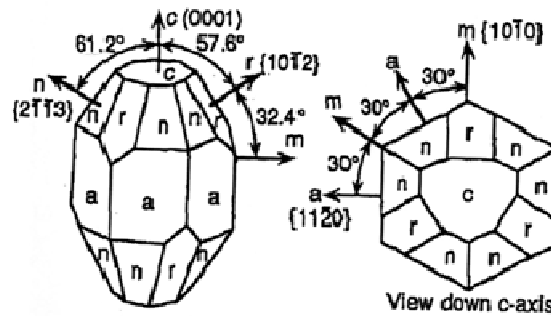
Fig. 2: Close-up view of test sample set-up for shadowgraphs

EOI IMPACT TEST RESULTS

Eight edge-on impact tests were performed in a shadowgraph optical arrangement. Five different orientations of the specimens' crystal axis and surfaces with respect to impact direction were considered. The test matrix is presented in Table I. The orientation of the different crystal planes and axis is illustrated in Figure 3.

TABLE I. EOI TEST MATRIX

Config. #	Impact Direction	Large Surface	Projectile	EMI Test #
1)	a-axis (parallel)	c-plane	sphere	17074
			cylinder	17071
2)	a-axis (parallel)	r-plane	sphere	17075
			cylinder	17069
3)	c-axis (parallel)	a-plane	sphere	17076
			cylinder	17070
4)	c-axis (perpendicular)	a-plane	sphere	17077
5)		Edge surface r-plane	sphere	17359

Figure 3 Saphire (α -Al₂O₃) crystal mineralogical nomenclature and Miller-index notation from Schmid and Harris [11]

Results Comparing Spherical with Cylindrical Impactors in Configuration 1)

1. SPHERE IMPACT

A selection of eight high-speed photographs from the impact of a steel sphere on the edge of a sapphire specimen at 453 m/s, parallel to the a-axis (large surface (0001)-plane), is presented in Figure 4.

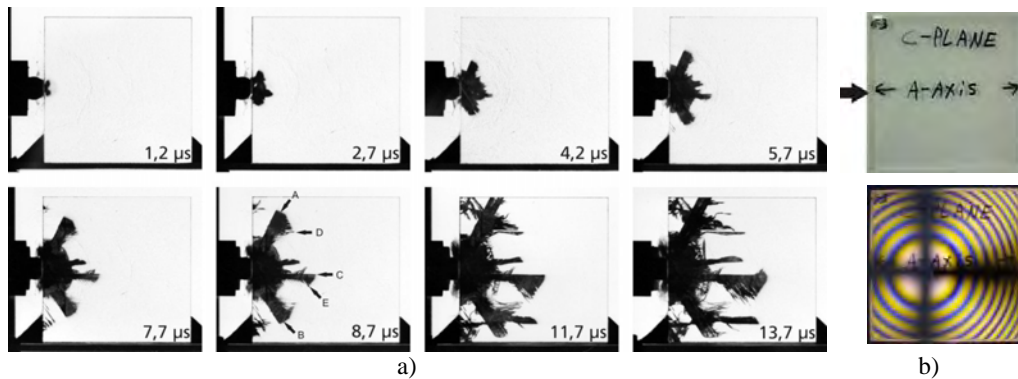


Figure 4. a) Selection of 8 high-speed shadowgraphs from impact with steel sphere, test # 17074

b) Plane light photograph of specimen before impact, illustrating the impact configuration (top) and conoscopic (viewed in crossed polars) interference figure photograph – note that the optical figure is not quite centered, meaning that the c-axis is not quite perpendicular to the a-axis plane.

The first cracks, possibly along prismatic cleavage planes, appeared immediately after impact, cutting a cone with an angle of about 120° into the specimen (fractures A, B). After $2.7 \mu\text{s}$ a third main fracture was visible, propagating straight in the impact direction (C). About eight microseconds later cracks branched off the cone cracks at an angle of about 60° , growing in the impact direction. From the central fracture C cracks also branched off at an angle of about -55° .

The path-time histories of the different fractures are shown in Figure 5. The fact, that the straight lines of the different fractures in Figure 5 are nearly parallel, demonstrates that all fractures propagated nearly at the same speed. The measured average velocities varied between 4590 m/s and 4934 m/s. For the sake of clarity in the presentation, arbitrary offsets were added to the coordinates of different fractures.

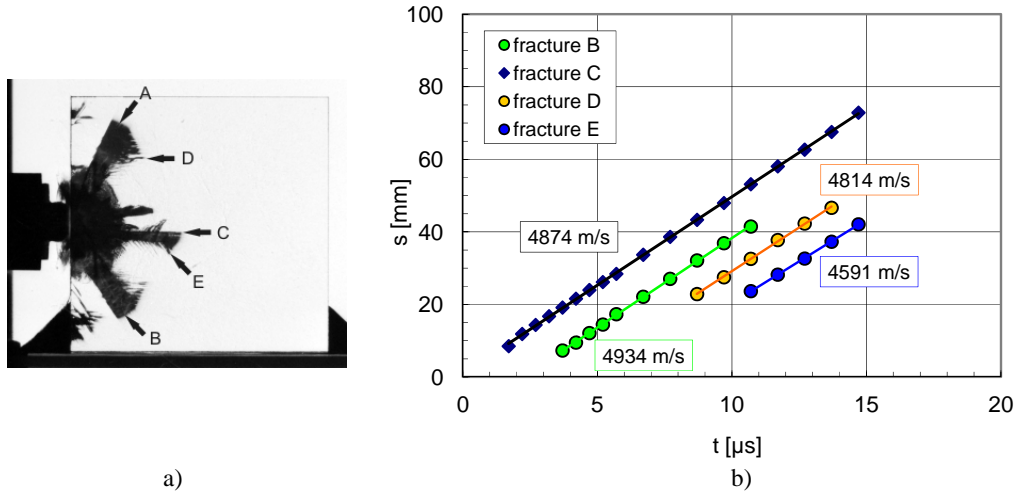


Figure 5. a) Nomenclature of fracture
b) Path-time history of fracture propagation, test no. 17074

2. CYLINDER IMPACT

In contrast to the impact of a steel sphere, where crack propagation occurred along certain crystal directions, the fracture pattern due to impact of a steel cylinder exhibited many similarities to the fracture patterns observed with the polycrystalline transparent ceramic AlON. This is illustrated by a selection of 8 high-speed photographs in Figure 6. The photograph at $1.2 \mu\text{s}$ after impact shows that crack formation starts along the edge of the projectile, where shear stresses are dominant. Only $3 \mu\text{s}$ later, a dense field of cracks has evolved in the zone ahead of the projectile, which develops a nearly semi-circular shape in the following. Due to the shear wave travelling along the impacted edge, a series of cracks were initiated consecutively above and below the projectile, forming the triangular shaped so-called secondary fracture zones. Nucleation and growth of crack centers appeared

throughout the period of observation so that the central fracture front propagated constantly at a high velocity.

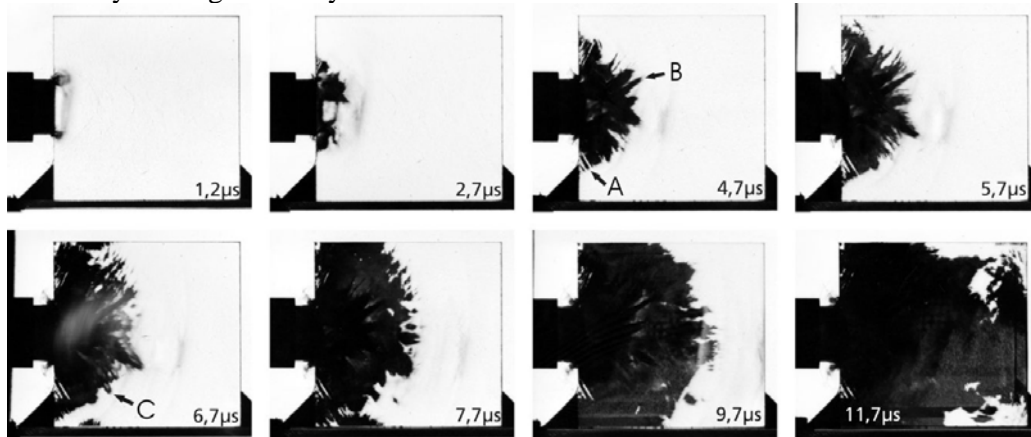


Figure 6. Selection of 8 high-speed shadowgraphs from impact with steel cylinder, test # 17071

The path-time histories of crack and wave propagation from test no. 17071 are plotted in Figure 7. A velocity of 11451 m/s was determined for the longitudinal wave from the shadowgraphs. The fracture front ahead of the projectile propagated at an average velocity of 8434 m/s and did not slow down during the period of observation. Cracks A and C grew at average speeds between 5200 m/s and 5700 m/s, whereas fracture B in the center propagated at about the same speed as the fracture front ($v_{\text{fracture C}} = 8137 \text{ m/s}$).

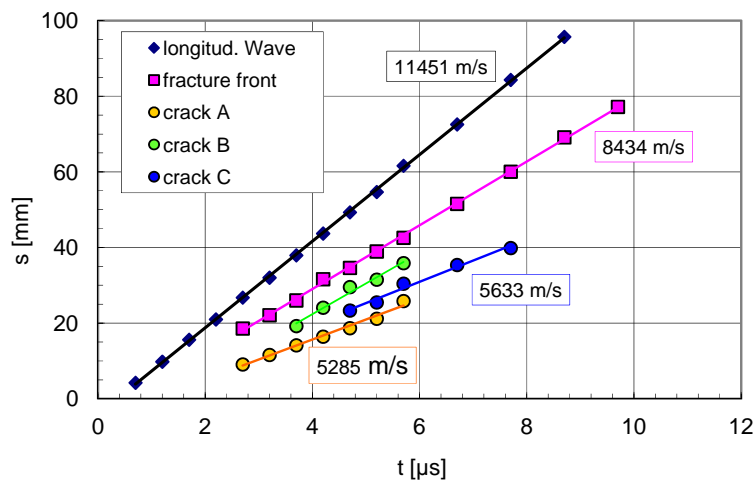


Figure 7. Path-time history of fracture propagation, test no. 17071

Comparison of Damage and Cleavage Controlled Crack Propagation

1. TEST # 17076: ORIENTATION 3), SPHERE IMPACT

In test no. 17076 the sapphire specimen was impacted by steel sphere at 456 m/s, parallel to the c-axis (large surface a-plane). Eight selected high-speed photographs are shown in Figure 8.

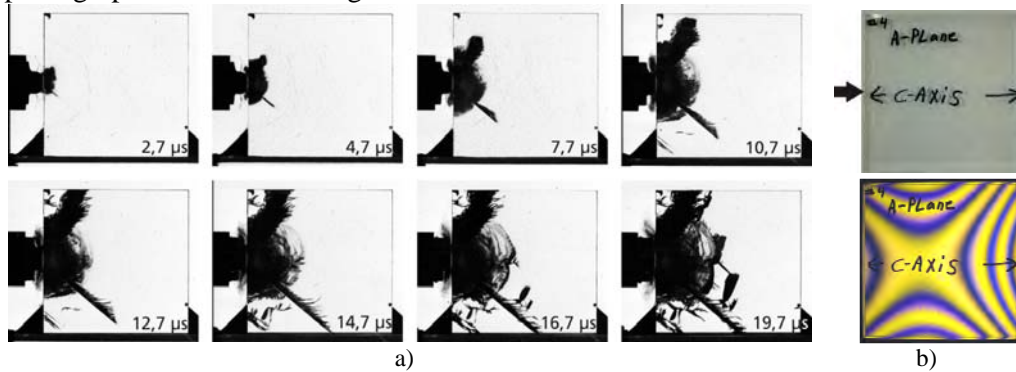
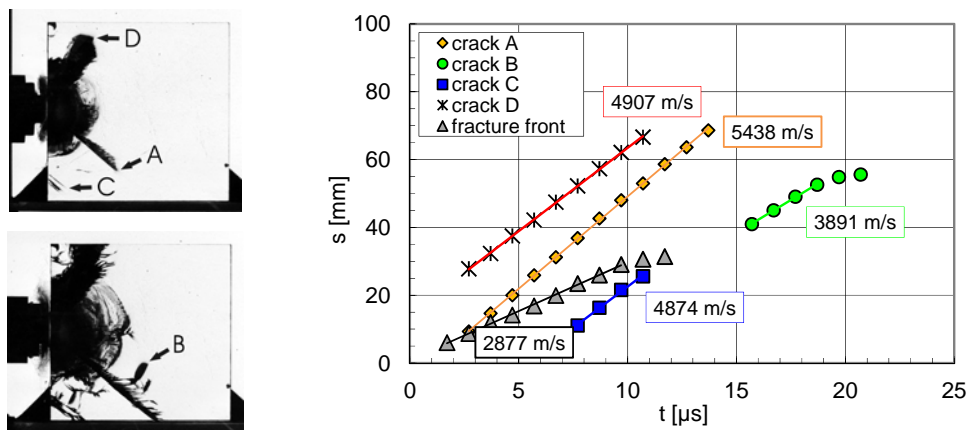


Figure 8. a) Selection of eight high-speed photographs from test # 17076 in orientation 3 at 456 m/s
b) Illustration of impact configuration (top) and optical interference figure (bottom)

In contrast to the other tests an asymmetric fracture pattern could be recognized from the shadowgraphs. Whereas one clearly recognizable crack propagated at -41° with respect to the impact axis, a bunch of cracks grew in the upper part of the specimen, forming a broad fracture path. A crack front, due to shell shaped fragments forming cracks, was observed in the center which stopped at about $12 \mu\text{s}$ after impact. The secondary cracks, generated at the impacted edge in the lower part of the specimen, propagated at angle of -36° with respect to the c-axis.

The nomenclature and path-time histories of the different cracks are shown in Figure 9. The highest crack velocity observed in this test was 5438 m/s with crack A. Fractures C and D, which also started from the impacted edge propagated at average velocities of about 4900 m/s. Crack B, which had branched off crack A, exhibited a propagation velocity of about 1000 m/s less than the other cracks. The semi-circular fracture front in the center started at a significantly lower velocity of 2877 m/s compared to the ~ 4900 m/s in test no. 17075 (see next section) and tailed off at longer times, suggesting that the cleavage controlled fracturing, with less energy required for propagation, diverted the available energy to the cleavage controlled cracks.



a)

b)

Figure 9. a) Nomenclature of fracture

b) Bulk damage and cleavage controlled crack velocities in test # 17076

Figure 10 illustrates four SEM micrographs of fracture surfaces from test no. 17076. It is clear from the fracture surfaces that cleavage controls the fracture down to the nano-scale.

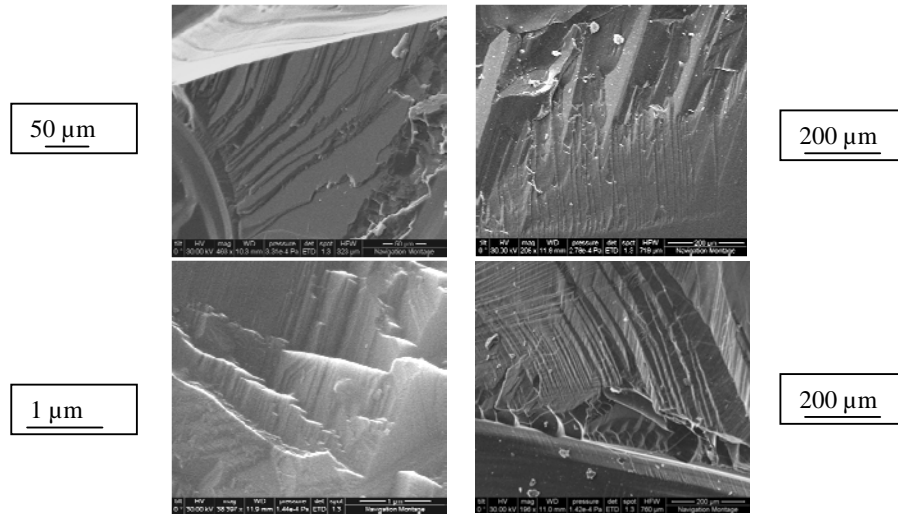


Figure 10. Four SEM micrographs of cleavage morphologies of fracture surfaces in test 17076.

2. TEST # 17075: ORIENTATION 2), SPHERE IMPACT

In this test, the sapphire specimen was impacted with a steel sphere, parallel to the a-axis (large surface r-plane) at 457 m/s. Figure 11 shows a selection of eight high-speed photographs and illustrates the impact configuration.

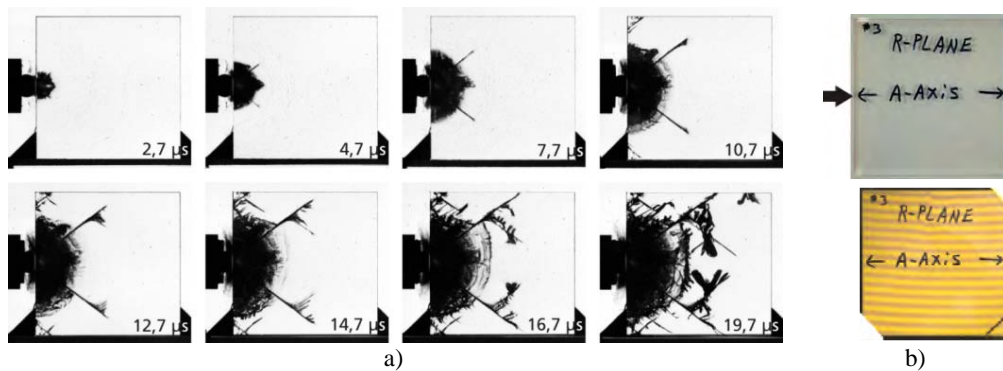


Figure 11. a) Selection of eight high-speed photographs from test # 17075 in orientation 2 at 457 m/s
b) Illustration of impact configuration (top) and optical interference figure (bottom)

Two main cracks were initiated (A, B), propagating at an angle of $\pm 37.5^\circ$ with respect to the a-axis. The black zone ahead of the projectile, which exhibited a nearly semi-circular shape after several microseconds, can be explained by the

formation of shell shaped cracks. After a few microseconds of crack growth parallel to the large surfaces these cracks grow towards the surface, cutting shell shaped fragments off the specimen. After 12.7 μs cracks (C) branching off the main cracks at an angle of 71.5° (34° with respect to a – axis) could be observed. The nomenclature of the analyzed cracks and the corresponding path-time histories are presented in Figure 12.

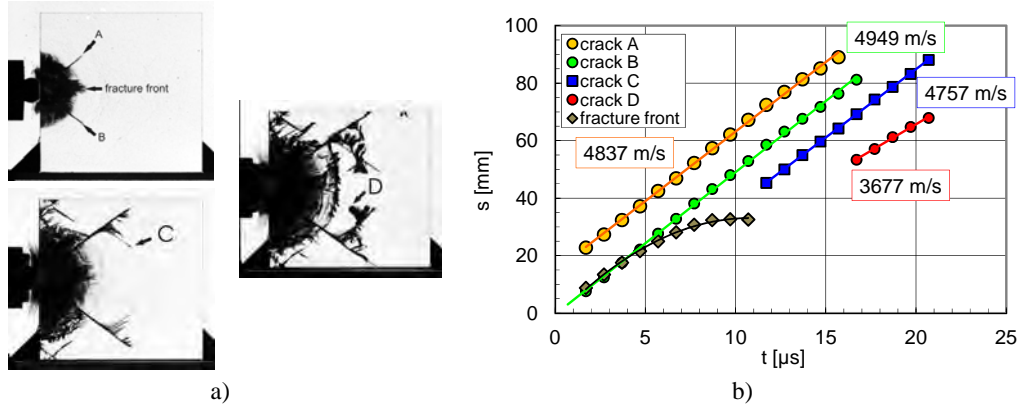
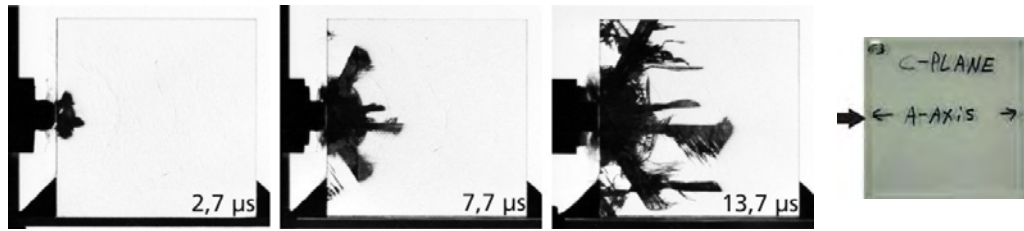


Figure 12. a) Nomenclature of fracture
b) Bulk damage and cleavage controlled crack velocities in test # 17075

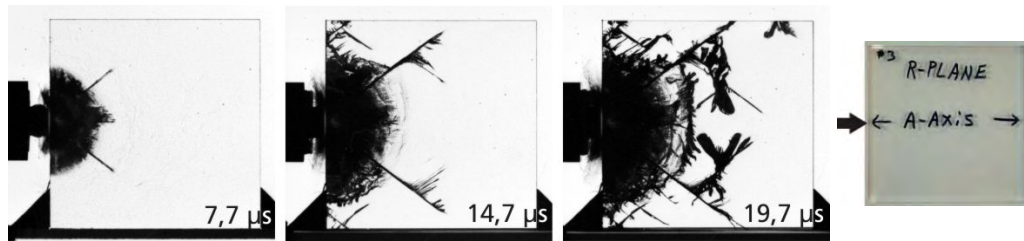
Linear regression of the path-time data from the main cracks A and B delivered nearly the same speed for both cracks: $v_{\text{crackA}} = 4837 \text{ m/s}$; $v_{\text{CrackB}} = 4949 \text{ m/s}$. For crack C, which branched off crack A at 71.5° , a slightly lower velocity of 4757 m/s was determined. Only crack D, which started from a side branch of crack B, propagated at a lower velocity of about 3700 m/s. The black fracture front in the center started at the same velocity as the main cracks, but slowed down after $\sim 5 \mu\text{s}$ and stopped after $\sim 10 \mu\text{s}$, similar to what was observed in test no. 17076. At this time the cracks, forming shell shaped fragments, have reached the surface of the specimen. For the sake of clarity in the presentation, arbitrary offsets were added to the coordinates of cracks A, and D.

3. DAMAGE AND CRACK MORPHOLOGIES FROM SPHERE IMPACT IN FIVE ORIENTATIONS

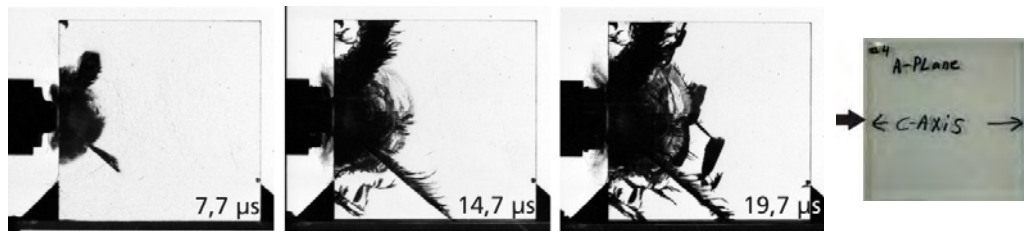
It is very clear from the high speed shaowgraphs in Figure 13 a-e, that the available cleavage planes can play a dominant role in controlling the fracture front when the energy available is not enough to propagate an undifferentiated damage zone.



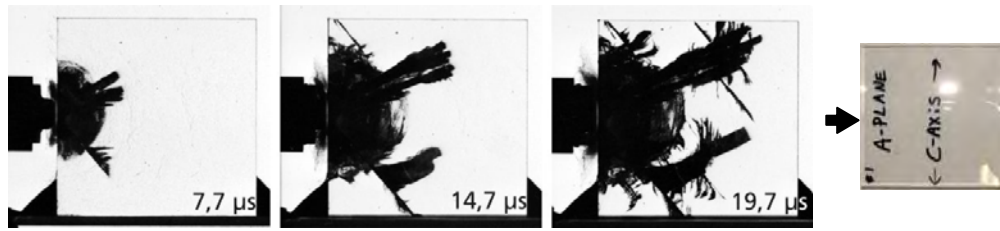
a) Orientation 1, 453 m/s, EMI Test #17074



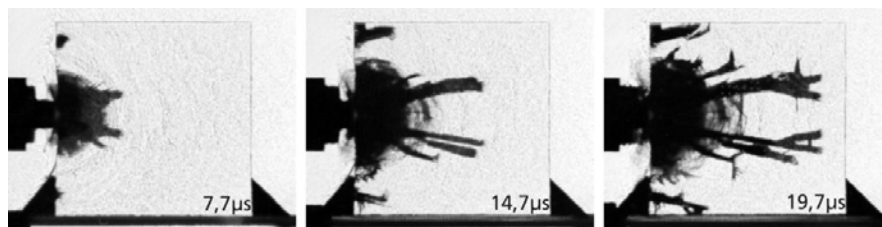
b) Orientation 2, 457 m/s, EMI Test #17075



c) Orientation 3, 456 m/s, EMI Test #17076



d) Orientation 4, 454 m/s, EMI Test #17077



e) Orientation 5, 451 m/s, EMI Test #17359. Impact edge is r-plane

Figure 13. Comparison of damage and crack morphologies

DISCUSSION

Bradt [12] has reviewed the cleavage and calculated energies for several cleavage planes of sapphire single crystals. The predominant cleavage planes are as follows: the c-plane (0001) basal plane; the r-plane ($10\bar{1}1$) rhombohedral plane and the m-plane ($10\bar{1}0$) prismatic plane. The theoretical surface energies at about 6.5 J/m^2 are almost equal for all three cleavage planes. However, the experimental K_{IC} toughness and cleavage energies are as follows: (0001) = $4.54 \text{ MPa m}^{1/2}$ and 21.54 J/m^2 ; ($10\bar{1}1$) = $2.38 \text{ MPa m}^{1/2}$ and 6.45 J/m^2 and ($10\bar{1}0$) = $3.14 \text{ MPa m}^{1/2}$ and 11.43 J/m^2 . This suggests that the energy to propagate a cleavage crack is most difficult along the (0001), followed by the ($10\bar{1}0$) and ($10\bar{1}1$) planes. It is well known that rhombohedral cleavage predominates in sapphire. Clayton [13] has recently reviewed continuum modeling theory for sapphire.

It is the author's view that the morphology of the damage front will be controlled by a competition between the available impact energy to create a massive undifferentiated damage front with the energy to have the damage controlled by the available properly oriented cleavage planes. The critical resolved shear stress (Schmid factor), which is a function of the angle between the loading direction and the cleavage plane and the applied load, will control the ease of formation of cleavage controlled cracks/damage or undifferentiated damage zones. Therefore, in some sapphire plate orientations damage will be dominated by cleavage and not in others.

In addition, it should be noted that the mass of the solid cylinder impactor (127 g) compared to the sphere impactor (39 g) means that at the same velocity the energy deposited by the solid cylinder is more than three times that of the sphere. In the solid cylinder case, since the available energy is much higher than the sphere the energy to propagate an undifferentiated massive damage has been exceeded and therefore, the available cleavage planes do not dominate the damage front morphology.

SUMMARY

Edge-on impact tests have been conducted with steel cylinders and spheres in order to generate a set of baseline data for fracture and wave propagation in Sapphire of different crystal orientation with respect to the direction of observation and shot axis. When the sapphire specimens were subjected to impact of steel cylinders fracture fronts were observed, similar to those in polycrystalline materials. In case of impact of spherical projectiles, fracture mainly followed cleavage planes of the crystal. The maximum average velocity observed for single cracks was 5438 m/s . The lowest crack velocities were about 3700 m/s .

ACKNOWLEDGMENTS

The work reported here was performed under a contract from the US Army International Technology Center - Atlantic (USAITC-A) supported by the U. S. Army Research Laboratory.

REFERENCES

1. Strassburger, E. 2009. "Ballistic testing of transparent armour ceramics", *Journal of the European Ceramic Society*, 29: 267-273
2. Patel, P.J., G.A. Gilde, P.G. Dehmer and J.W. McCauley. 2000. "Transparent Armor", *AMPTIAC Quarterly* 4(3): 1-6
3. Patel, P.J. and G.A. Gilde. 2002. "Transparent Armor Materials: Needs and Requirements", *Ceramic Armor Materials by Design*, *Ceramic Transactions* 134: 573-586
4. Jones, C.D., J.B. Rioux, J.W. Locher, H.E. Bates, S.A. Zanella, V. Pluen and M. Mandelartz. 2006. "Large-Area Sapphire for Transparent Armor", *American Ceramic Society Bulletin* 85(3): 24-26
5. Jones, C.D., J.B. Rioux, J.W. Locher, H.E. Bates, S.A. Zanella, V. Pluen and M. Mandelartz. 2008. "Ballistic Performance of Commercially Available Saint-Gobain Sapphire Transparent Armor Composites", *Advances in Ceramic Armor III*, *Ceramic Engineering and Science Proceedings* 28(5): 113-124
6. Strassburger, E., M. Hunzinger and A. Krell. 2010. "Fragmentation of Ceramics under Ballistic Impact", *Proc. of 25th Int. Symposium on Ballistics*: 1172-1179
7. Shockey, D.A., D. Bergmannshoff, D.A. Curran and J.W. Simons. 2009. "Physics of Glass Failure during Rod Penetration", *Advances in Ceramic Armor IV*, *Ceramic Engineering and Science Proceedings* 29(6): 23-32
8. Strassburger E., P. Patel, J.W. McCauley and D.W. Templeton. 2007. "Wave Propagation and Impact Damage in Transparent Laminates", *Proc. of 23rd Int. Symposium on Ballistics*: 1381-1388
9. Strassburger, E., P. Patel, J.W. McCauley and D.W. Templeton. 2005. "High-Speed Photographic Study of Wave and Fracture Propagation in Fused Silica", *Proc. 22nd Int. Symposium on Ballistics*: 761-768
10. Strassburger, E., P. Patel, J.W. McCauley and D.W. Templeton. 2005. "Visualization of Wave Propagation and Impact Damage in a Polycrystalline Transparent Ceramic – AION", *Proc. 22nd Int. Symp. on Ballistics*: 769-776
11. Schmid, F., and D.C. Harris. 1998. "Effects of Crystal Orientation and Temperature on the Strength of Sapphire", *J. Am. Ceram. Soc.* 81(4): 885-893
12. Bradt, R. "Cleavage of Ceramic and Mineral Single Crystals", *George R. Irwin Symposium*, *Proceedings of a symposium at the Sept. 15-17, 1997 TMS Meeting, Indianapolis, Indiana*.
13. Clayton, J. "Finite Deformations by Elasticity, Slip, and Twinning: Atomistic Considerations, Continuum Modeling, and Application to Ceramic Crystals", *ARL-RP-244*, March 2009.

NO. OF
COPIES ORGANIZATION

1 DEFENSE TECHNICAL
(PDF INFORMATION CTR
only) DTIC OCA
8725 JOHN J KINGMAN RD
STE 0944
FORT BELVOIR VA 22060-6218

1 DIRECTOR
US ARMY RESEARCH LAB
IMNE ALC HRR
2800 POWDER MILL RD
ADELPHI MD 20783-1197

1 DIRECTOR
US ARMY RESEARCH LAB
RDRL CIO LL
2800 POWDER MILL RD
ADELPHI MD 20783-1197

1 DIRECTOR
US ARMY RESEARCH LAB
RDRL CIO MT
2800 POWDER MILL RD
ADELPHI MD 20783-1197

1 DIRECTOR
US ARMY RESEARCH LAB
RDRL D
2800 POWDER MILL RD
ADELPHI MD 20783-1197

NO. OF
COPIES ORGANIZATION

1 ODUSD (SANDT) WS
L SLOTER
ROSSLYN PLAZA N
STE 9030
1777 N KENT ST
ARLINGTON VA 22209-2210

1 COMMANDER
US ARMY MATL CMND
AMXMI INT
9301 CHAPEK RD
FORT BELVOIR VA 22060-5527

1 PEO GCS
SFAE GCS BCT/MS 325
M RYZYI
6501 ELEVEN MILE RD
WARREN MI 48397-5000

1 ABRAMS TESTING
SFAE GCSS W AB QT
J MORAN
6501 ELEVEN MILE RD
WARREN MI 48397-5000

1 COMMANDER
WATERVLIET ARSENAL
SMCWV QAE Q
B VANINA
BLDG 44
WATERVLIET NY 12189-4050

2 COMMANDER
US ARMY AMCOM
AVIATION APPLIED TECH DIR
J SCHUCK
FORT EUSTIS VA 23604-5577

1 NVL SURFC WARFARE CTR
DAHLGREN DIV CODE G06
DAHLGREN VA 22448

1 USA SBCCOM PM SOLDIER SPT
AMSSB PM RSS A
J CONNORS
KANSAS ST
NATICK MA 01760-5057

2 UNIV OF DELAWARE
DEPT OF MECH ENGR
J GILLESPIE
NEWARK DE 19716

NO. OF
COPIES ORGANIZATION

3 AIR FORCE ARMAMENT LAB
AFATL DLJW
W COOK
D BELK
J FOSTER
EGLIN AFB FL 32542

1 DPTY ASSIST SCY FOR R&T
(CD SARD TT
only) ASA (ACT)
J PARMENTOLA
THE PENTAGON RM 3E479
WASHINGTON DC 20310-0103

1 US ARMY TACOM ARDEC
AMSRD AAR AEE W
E BAKER
BLDG 3022
PICATINNY ARSENAL NJ
07806-5000

11 US ARMY TARDEC
AMSTRA TR R MS 263
K BISHNOI
D TEMPLETON (10 CPS)
WARREN MI 48397-5000

1 COMMANDER
US ARMY RSRCH OFC
A RAJENDRAN
PO BOX 12211
RSRCH TRIANGLE PARK NC
27709-2211

2 CALTECH
G RAVICHANDRAN
T AHRENS MS 252 21
1201 E CALIFORNIA BLVD
PASADENA CA 91125

5 SOUTHWEST RSRCH INST
C ANDERSON
K DANNEMANN
T HOLMQUIST
G JOHNSON
J WALKER
PO DRAWER 28510
SAN ANTONIO TX 78284

3 SRI INTERNATIONAL
D CURRAN
D SHOCKEY
R KLOOP
333 RAVENSWOOD AVE
MENLO PARK CA 94025

NO. OF
COPIES ORGANIZATION

1 APPLIED RSRCH ASSOC
D GRADY
4300 SAN MATEO BLVD NE
STE A220
ALBUQUERQUE NM 87110

1 INTERNATIONAL RSRCH
ASSOCIATES INC
D ORPHAL CAGE 06EXO
4450 BLACK AVE
PLEASANTON CA 94566

1 BOB SKAGGS CONSULTANT
S R SKAGGS
7 CAMINO DE LOS GARDUNOS
SANTA FE NM 87501

2 WASHINGTON ST UNIV
INST OF SHOCK PHYSICS
Y GUPTA
J ASAY
PULLMAN WA 99164-2814

1 COORS CERAMIC CO
T RILEY
600 NINTH ST
GOLDEN CO 80401

1 UNIV OF DAYTON
RSRCH INST
N BRAR
300 COLLEGE PARK
MS SPC 1911
DAYTON OH 45469-0168

2 COMMANDER
US ARMY TACOM
AMSTA TR S
T FURMANIAK
L PROKURAT FRANKS
WARREN MI 48397-5000

1 PM HBCT
SFAE GCS HBCT S
J ROWE MS 506
6501 E 11 MILE RD
WARREN MI 48397-5000

1 NVL SURFC WARFARE CTR
CARDEROCK DIVISION
R PETERSON
CODE 28
9500 MACARTHUR BLVD
WEST BETHESDA MD 20817-5700

NO. OF
COPIES ORGANIZATION

3 COMMANDER
US ARMY RSRCH OFC
B LAMATINA
D STEPP
W MULLINS
PO BOX 12211
RSRCH TRIANGLE PARK NC
27709-2211

2 LAWRENCE LIVERMORE NATL LAB
R LANDINGHAM L369
J E REAUGH L282
PO BOX 808
LIVERMORE CA 94550

4 SANDIA NATL LAB
J ASAY MS 0548
L CHHABILDAS MS 0821
D CRAWFORD ORG 0821
M KIPP MS 0820
PO BOX 5800
ALBUQUERQUE NM 87185-0820

3 RUTGERS
THE STATE UNIV OF NEW JERSEY
DEPT OF CRMCS & MATLS ENGRNG
R HABER
607 TAYLOR RD
PISCATAWAY NJ 08854

2 THE UNIVERSITY OF TEXAS
AT AUSTIN
S BLESS
IAT
3925 W BRAKER LN STE 400
AUSTIN TX 78759-5316

3 SOUTHWEST RSRCH INST
C ANDERSON
J RIEGEL
J WALKER
6220 CULEBRA RD
SAN ANTONIO TX 78238

1 CERCOM
R PALICKA
991 PARK CENTER DR
VISTA CA 92083

1 JET PROPULSION LAB
IMPACT PHYSICS GROUP
M ADAMS
4800 OAK GROVE DR
PASADENA CA 91109-8099

NO. OF
COPIES ORGANIZATION

6 GDLS
W BURKE MZ436 21 24
G CAMPBELL MZ436 30 44
D DEBUSSCHER MZ436 20 29
J ERIDON MZ436 21 24
W HERMAN MZ435 01 24
S PENTESCU MZ436 21 24
38500 MOUND RD
STERLING HTS MI 48310-3200

3 OGARA HESS & EISENHARDT
G ALLEN
D MALONE
T RUSSELL
9113 LE SAINT DR
FAIRFIELD OH 45014

2 CERADYNE INC
M NORMANDIA
3169 REDHILL AVE
COSTA MESA CA 96626

3 JOHNS HOPKINS UNIV
DEPT OF MECH ENGRNG
K T RAMESH
3400 CHARLES ST
BALTIMORE MD 21218

2 SIMULA INC
V HORVATICH
V KELSEY
10016 51ST ST
PHOENIX AZ 85044

3 UNITED DEFNS
LIMITED PARTNERS
GROUND SYS DIV
E BRADY
R JENKINS
K STRITTMATTER
PO BOX 15512
YORK PA 17405-1512

10 NATL INST OF STANDARDS & TECH
CRMCS DIV
G QUINN
STOP 852
GAITHERSBURG MD 20899

2 DIR USARL
AMSRD ARL D
C CHABALOWSKI
V WEISS
2800 POWDER MILL RD
ADELPHI MD 20783-1197

NO. OF
COPIES ORGANIZATION

ABERDEEN PROVING GROUND

62 DIR USARL
RDRL SL
R COATES
RDRL WM
S KARNA
J MCCAULEY (20 CPS)
T WRIGHT
RDRL WML
J NEWILL
M ZOLTOSKI
RDRL WML H
T FARRAND
L MAGNESS
D SCHEFFLER
R SUMMERS
RDRL WMM
R DOWDING
RDRL WMM A
S MCKNIGHT
J SANDS
RDRL WMM B
G GAZONAS
RDRL WMM D
E CHIN
K CHO
R SQUILLACIOTI
RDRL WMM E
J LASALVIA
P PATEL
RDRL WMM F
J MONTGOMERY
RDRL WMP
P BAKER
B BURNS
S SCHOENFELD
RDRL WMP B
C HOPPEL
J CLAYTON
D DANDEKAR
M GREENFIELD
M SCHEIDLER
T WEERASOORIYA
RDRL WMP C
T BJERKE
S SEGLETES
W WALTERS
RDRL WMP D
T HAVEL
M KEELE
D KLEPONIS
H MEYER
J RUNYEON

NO. OF
COPIES ORGANIZATION

RDRL WMP E
T JONES
P BARTKOWSKI
M BURKINS
W GOOCH
D HACKBARTH
E HORWATH

NO. OF
COPIES ORGANIZATION

3 FRAUNHOFER-INSTITUT FÜR
KURZZEITDYNAMIK (EMI)
PROF DR K THOMA
DIPL-PHYS E STRAßBURGER
AM KLINGELBERG 1 D – 79588
EFRINGEN-KIRCHEN
GERMANY

INTENTIONALLY LEFT BLANK.